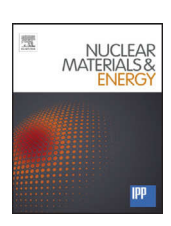
ELSEVIER

Contents lists available at ScienceDirect

Nuclear Materials and Energy

journal homepage: www.elsevier.com/locate/nme



Damaging of tungsten and tungsten-tantalum alloy exposed in ITER ELM-like conditions



V.A. Makhlai^{a,*}, I.E. Garkusha^a, J. Linke^b, S.V. Malykhin^c, N.N. Aksenov^a, O.V. Byrka^a, S.S. Herashchenko^a, S.V. Surovitskiy^c, M. Wirtz^b

- ^a Institute of Plasma Physics of the NSC KIPT, 61108 Kharkov, Ukraine
- ^b Forschungszentrum Julich, EURATOM Association, 52425 Julich, Germany
- ^c Kharkov Polytechnic Institute, NTU, 61002, Kharkov, Ukraine

ARTICLE INFO

Article history: Received 13 November 2015 Revised 31 March 2016 Accepted 1 April 2016 Available online 20 April 2016

PACS: 52.40.Hf

Keywords: Plasma-materials interaction Tungsten Surface effects Divertor materials

ABSTRACT

The damage of deformed double forged pure tungsten (W) and tungsten alloyed with 5 wt% tantalum (WTa5) have been studied in experimental simulations of ITER-like transient events with relevant surface heat load parameters (energy density up to 0.75 MJ/m² and the pulse duration of 0.25 ms) as well as particle loads (varied in wide range from 10²3 to 10²7 ion/m² s) with quasi-stationary plasma accelerator QSPA Kh-50. The plasma exposures were performed for the targets maintained at room temperature and preheated at 200 °C. The surface heat loads were either with no melting of W surface or above the melting threshold. The development of surface morphology of the exposed targets as well as cracking and swelling at the surface is discussed. Surface analysis was carried out with an optical microscopy and SEM. Surface modification and development of cracks led to increases of roughness of exposed surfaces. X-ray diffraction (XRD) has been used to study the micro-structural evolution of the exposed targets. The micro deformations of W and WTa5 are similar for targets exposed under similar conditions. The contribution of excess complexes of interstitial atoms in the formation of cracks after plasma irradiation was evaluated.

© 2016 The Authors. Published by Elsevier Ltd. This is an open access article under the CC BY-NC-ND license (http://creativecommons.org/licenses/by-nc-nd/4.0/).

1. Introduction

Tungsten is primary Plasma Facing Materials (PFC) for ITER divertor due to advantageous properties: high thermal conductivity, high temperature strength and stability, high recrystallization temperature and high spattering threshold for hydrogen [1,2]. Main disadvantage of tungsten is high brittleness. Alloying and forming of solid solutions are ways for ductilization of tungsten. Tantalum is one of elements (other ones rhenium, vanadium, molybdenum, titanium) which can create a solid solution with tungsten. However, solid solution of W-Ta can be more brittle than pure tungsten [2]. Nevertheless, thermal shock tests with e-beams fulfilled in JU-DITH [1,3] and hydrogen loading in GLADIS [2] facilities shown that W-Ta alloys have much better erosion properties.

Studies of erosion features, cracks evolution and changes in surface layers are also observed in quasi-stationary accelerators for

different W grades [4-8]. Application of quasi-stationary accelerators for heat load test of ITER-like plasma facing materials allows reproducing the heat and particle loads to the divertor surfaces that are expected in fusion reactor during transient events such as disruptions and Edge Localized Modes [4,9]. Two different crack meshes are identified after the exposure of the different tungsten kinds (sintered, rolled and deformed ones) with plasma streams. Major cracks appear due to ductile-to-brittle transition effects and do not depend on the tungsten grade. Inter-granular micro-cracks are detected at energy loads above the melting threshold. Distinct droplets of the melted materials were observed on the exposed surface under these conditions [9–11]. The blister-like and cellular-like structures were observed on the exposed surfaces. The deformed tungsten is found to be more resistant against cracking in comparison with other grades [6–8]. First experiments studying the erosion features on double forged pure tungsten and WTa5 alloy exposed by plasma streams were also performed. Among studied tungsten grades WTa5 shows better performance in terms of cracks for small number of plasma loads. Only single isolated

^{*} Corresponding author. Tel. +380573356305. E-mail address: makhlay@ipp.kharkov.ua (V.A. Makhlai).

cracks which do not form the complete mesh on the surface are registered after plasma exposures [8].

Accumulation and comparison data from a number of very different test facilities (electron, ion and plasma) might be a basis for choosing the material with much better properties. For this reason, the main objective of this work is to study the features of macroscopic erosion of the pure tungsten and tungsten–tantalum alloy irradiated by plasma streams in powerful plasma accelerator QSPA Kh-50. It is considered as important direction of experimental studies of damages of different grades of tungsten as major plasma facing material relevant to ITER and DEMO.

2. Experimental device and diagnostics

Heat load tests of tungsten and tungsten–tantalum alloy with energy density, pulse duration and particle loads relevant to ITER transient events have been carried out in a quasi-stationary plasma accelerator QSPA Kh-50 [9]. The main parameters of the hydrogen plasma streams are as follows: ion impact energy about 0.4 keV, maximum plasma pressure 0.32 MPa, and the stream diameter 18 cm. The plasma pulse shape is approximately triangular, pulse duration 0.25 ms [9]. The surface energy loads measured with a calorimeter were 0.45 MJ/m² (below tungsten melting threshold (0.6 MJ/m²)) and 0.75 MJ/m² (resulting in melting of tungsten surface) [5,7,10].

Surface analysis of exposed samples was carried out with an optical microscope MMR-4 equipped with a CCD camera and Scanning Electron Microscope (SEM) JEOL JSM-6390. Measurements of weight losses and precise measurements of the surface roughness with the Hommelwerke tester T500 were also performed.

X-ray diffraction (XRD) has been used to study structure, substructure and stress state of targets. 9–29 scans were performed using a monochromatic Cu- $K\alpha$ radiation [11,12]. Computer processing of the experimental diffraction patterns was performed using the New profile 3.5 software package. The analysis of diffraction peaks intensity, profiles, width (B), angular positions were applied to evaluate texture, coherent scattering region size. Changes of phase state on the surface were obtained from XRD spectrum analysis (Fig. 1).

For evaluation of changes of structure and sub-structure state, the peak (400) was used, located in the precision area of angles (Fig. 2). Generally, the width (B) of the profile is proportional to the number of line defects (dislocations) in the structure. According to the theory of scattering [11] the diffraction peak should be symmetrical. Asymmetrical profile can be considered as superposition of two symmetrical peaks. One of them is the theoretical main peak and second diffusion maximum is associated with defects of the structure. The asymmetry parameter (δB) was given for quantitative characteristics of asymmetry as: $\delta B = (B_{left} - B_{right})/(B_{left} + B_{right})$, where B_{left} . – left part of width at half-height, B_{right} – right part of width at half-height. The asymmetry ($\delta B \neq 0$) is attributed by the presence of complexes of point defects. The sign of δB is caused by the type of defects: vacancies ($\delta B > 0$) (in other words diffusion maximum appear on left from main) or interstitial atoms ($\delta B < 0$) (i.e. diffusion maximum on right from main).

Residual macro-stresses (σ) and the lattice parameter in the stress free state (a_0) were determined using a-sin $^2\psi$ -plots [11–14] by the peaks (400) located in the precision area of angles (Fig. 3). Dashed line showed the stress free cross section according to which a_0 was determined. If lattice parameter in the stress free state (a_0) is less than the corresponding reference value $(a_{\rm ref}=0.3165~{\rm nm})$ then a lot of vacancies are present in structure. If $a_0>a_{\rm ref}$ the surplus interstitial atoms are observed in structure. It can be also attributed to alloying of tungsten by heavy elements.

Analysis of the average coherence length (associated with the density of dislocation in the boundaries of grains) and the value

of the average micro strain (density of chaotically distributed dislocations inside the coherence length) has been carried out by the approximation method [9,13,14].

3. Characterization of initial state of studied samples

Double forged samples of pure tungsten (W) and tungsten alloyed with 5 wt% tantalum (WTa5) were used for the plasma loads tests. Samples have sizes of $12 \times 12 \times 5$ mm³. All samples were supplied by Plansee AG (Austria), prepared and delivered from Forschungszentrum Julich (Germany) [3]. Before each plasma pulse, the surface temperature of one part of targets had been near room temperature (RT). Other part of samples had been preheated to $200\,^{\circ}\text{C}$ with special heater [5]. It should be mentioned that even at this temperature double forged pure tungsten and WTa5 alloy have shown high cracking resistance in experiments with JUDITH 1 facility [3].

All perpetrated samples had very small initial surface roughness (R $_a\approx 0.1~\mu m$, R $_z\approx 0.4~\mu m$, R $_{max}\approx 0.5~\mu m$). The samples of pure W and WTa5 have texture of [200] (Fig. 1.). Such texture is analog of [100]. The compressive residual macro stresses of (–170 to –40) MPa was registered in surface layers of W and WTa5 targets in initial state.

For pure tungsten: lattice parameter $a_0 < a_{\rm ref}$ (Fig. 3a) i.e. excess vacancies presents in structure. It agrees with sign of asymmetry parameter $(\delta B \approx (2-5)\%>0)$ associated with excess number of vacancies complex. Width of diffraction line in pure tungsten is $B \approx (8.7-9.8)\times 10^{-3}$ rad that is near width of line (400) in material with perfect structure [13].

WTa5 alloy is characterized by $a_0 \approx 0.317 \text{ nm} > a_{\text{ref}}$ (Fig. 3b) due to presence of surplus interstitial (alloying) atoms. $B \approx 12 \times 10^{-3}$ rad indicates a large number of linear defects for WTa5. Asymmetry of such samples was near zero ($\delta B \approx -0.2\%$) and probably associated with excess number of complex interstitial atoms.

It should be mentioned, that the average size of coherent area is practically the same (300–400 nm) for pure tungsten and WTa5. Dislocation density in inside of pure tungsten grains was estimated as $\rho_{\varepsilon} \approx 4.6 \times 10^{10} \ \mathrm{cm^{-2}}$. For WTa5 alloy $\rho_{\varepsilon} \approx 2.6 \times 10^{10} \ \mathrm{cm^{-2}}$. For both kinds of samples the density of dislocations in boundaries achieved $\rho_{\mathrm{I}} \approx 2.5 \times 10^{11} \ \mathrm{cm^{-2}}$.

4. Experimental results and discussion

Surface pattern, damage and structure of pure tungsten and tungsten-tantalum alloy WTa5 targets have been analyzed in condition of preheating to 200 °C and at room temperature (RT). Plasma loads up to 100 pulses below the melting threshold and also in conditions of pronounced melting were performed.

4.1. Common feature of pure W and WTa5 exposed to plasma streams

The XRD diffraction analysis has confirmed absence of material phases built of impurities on the surface of all studied samples. Only tungsten lines on the surface and in deeper layers were observed. After plasma exposes texture of all studied samples did not changes and improved (Fig. 1). Asymmetry become negative and rose with increasing of number of pulses. Width of diffraction profiles (i.e. average dislocation density) weakly changes in surface layer. The average size of coherent area, average dislocation density both in boundaries and in inside of grains did not changes.

For heat load above melting threshold both major cracks and micro-cracks network along the grain boundaries is always detected in experiments independently of surface temperature before irradiation (Fig. 4 and Fig. 5). It is attributed to the surface melting

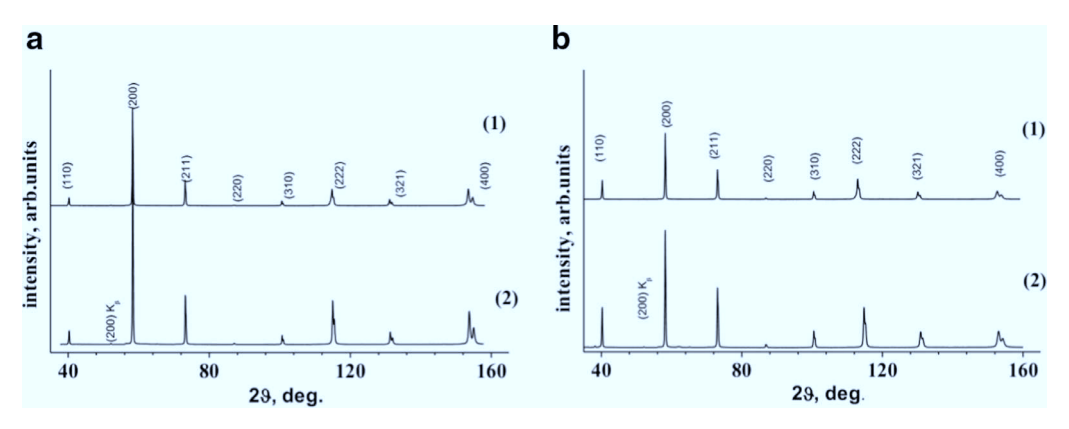


Fig. 1. Diffraction patterns (Cu-Kα radiation) of pure tungsten (a) and WTa5 alloy (b): initial state (1) and after plasma exposure with 100 plasma pulses of 0.45 MJ/m² (2).

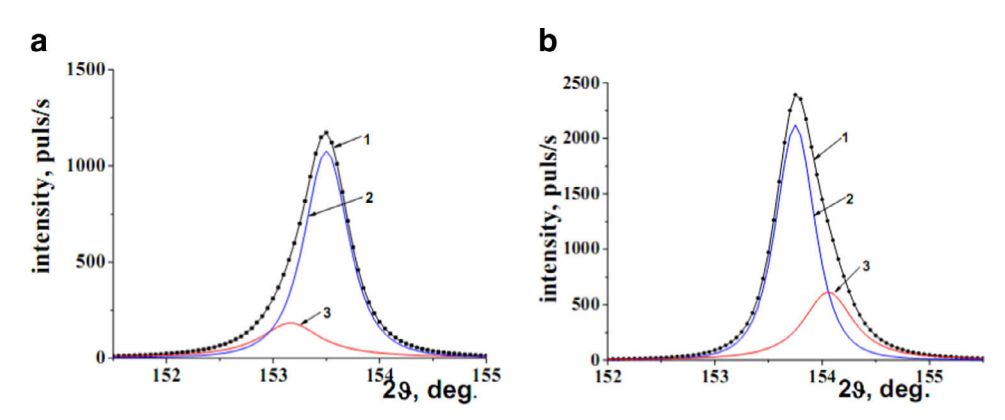


Fig. 2. Diffraction peak asymmetry with additional diffuse maximum before irradiation (a) and after plasma irradiation (b); experimental diffraction peak (1), main diffraction peak after computer processing (2), additional diffuse maximum (3).

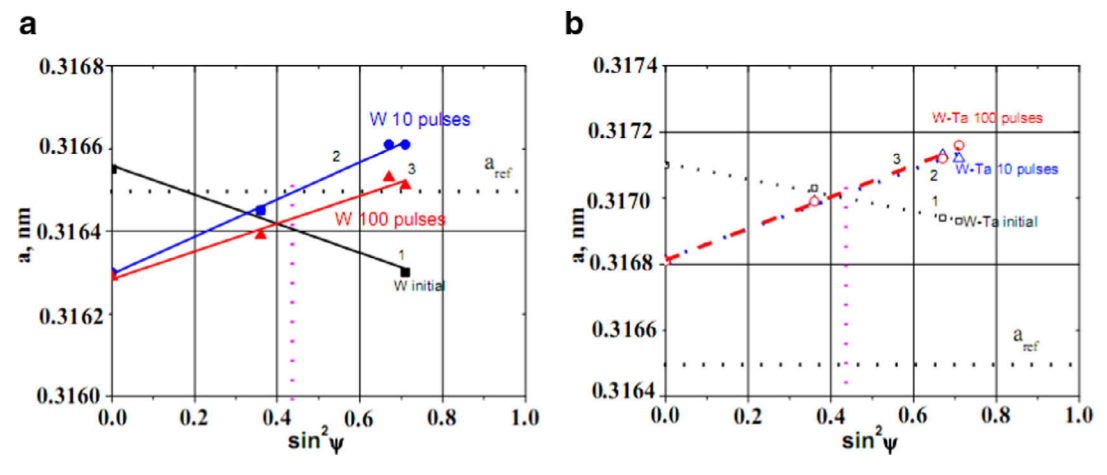


Fig. 3. Examples of a-sin2 ψ -plots for the sample of pure tungsten (a) and WTa5 alloy in the initial state (1) and after irradiation by 10 (2) and 100 (3) plasma pulses of 0.45 MJ/m².

and following resolidification. Typical cell sizes of intergranular micro-cracks network are within 10–40 μ m. Surface roughness after plasma exposures with surface melting is essentially higher in comparison with initial roughness and similar for W and WTa5 (Fig. 6). Fluctuation large peaks on profilograms correspond to the average distance between developed major cracks. Special surface morphology is developed due to the cracks networks appearance on the surface. It is influence of created melt layer and effects of surface tension.

Plasma irradiation results in a symmetrical tensile stress in thin subsurface layer. Maximal residual stress in the plasma affected layer is reached after first plasma pulses.

Mass loss measurements demonstrate growing erosion with increasing energy load as in previous experiments [9]. For targets irradiated with heat load below melting threshold, mass losses mainly can be caused by sputtering. The surface melting leads to splashing of eroded material.

4.2. Feature of pure W exposed plasma streams

Network of macro cracks developed on the surface pure tungsten irradiated with 10 pulses of 0.45 MJ/m² at initial surface temperature of RT (Fig. 7a). Rise of irradiation pulses number led to some growth of cracks width and splitting of crack mesh (Fig. 7b).

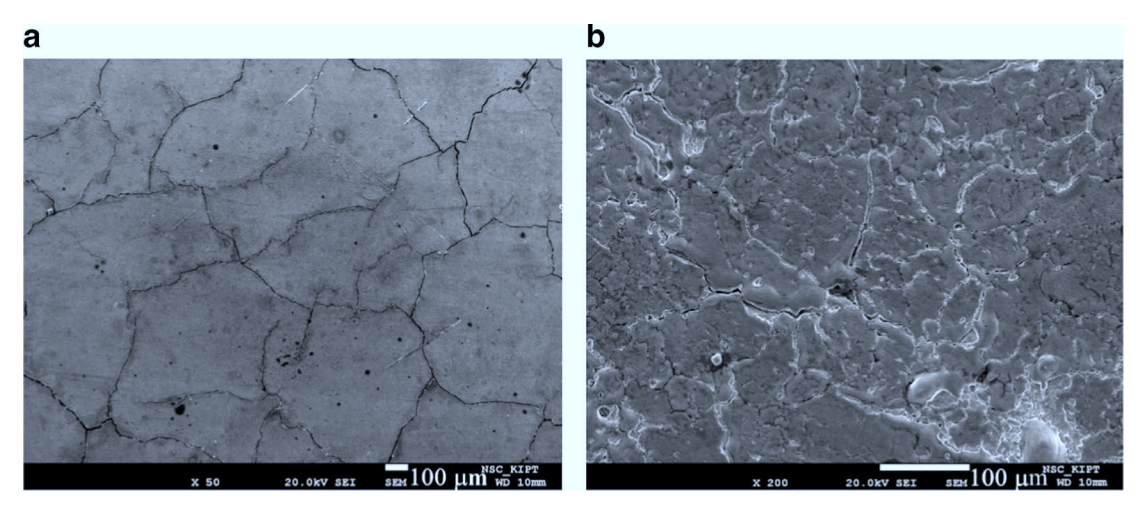


Fig. 4. SEM images of the W tungsten surface exposed to 100 plasma pulses of $0.75 \, MJ/m^2$ each for different initial surface temperature (Tin): Tin =RT (a) and Tin= $200 \, ^{\circ}$ C (b). The length of the white marker line is $100 \, \mu m$.

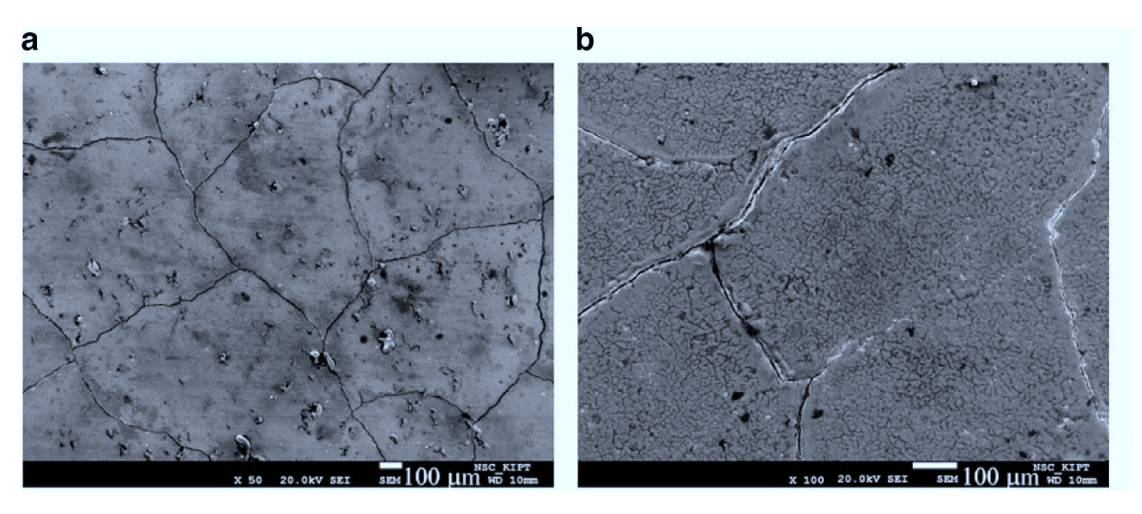


Fig. 5. SEM images of the WTa5 alloy surface exposed to 100 plasma pulses of $0.75 \, \text{MJ/m}^2$ each for different initial surface temperature (Tin): Tin =RT (a) and Tin= $200 \, ^{\circ}\text{C}$ (b). The length of the white marker line is $100 \, \mu m$.

Only few isolated cracks have appeared in some areas on the preheated surface exposed with heat load below melting threshold (Fig. 7c). With further increasing number of plasma pulses both width and depth of cracks some increased but new cracks did not appear (Fig. 7d). Cracks and growth of some edges of grains caused the development of a characteristic surface profile (Fig. 8.a).

Measurements demonstrate that the maximal value (300–400 MPa) of residual stress in thin subsurface layer does not depend practically on initial target temperature and it significantly grows with increasing thermal loads. Increasing the number of plasma pulses leads to some relaxation of residual stress (Fig. 3a). Preheating of surface contribute to faster relaxation of residual stresses. Surface melting of preheating surface causes the largest speed relaxation of residual stresses.

4.3. Feature of WTa5 exposed plasma streams

Only separate major cracks appear on surfaces with initial temperature of RT after first plasma pulses of 0.45 MJ/m² (Fig. 9a). With further increasing of irradiation pulses the width of cracks rises but the network of cracks does not develops (Fig. 9b). Thus, for heat load below melting threshold without preheating, the samples of WTa5 alloy demonstrated better resistance in comparison with pure tungsten [8].

Corrugated structure of hills and cracks appear after first plasma pulses with heat load below melting threshold on preheated surfaces (Fig. 9c). Width and depth of crack grow with increasing of number of pulses (Fig. 9d). Some exfoliation of surface layer on the separate parts of exposed surface is observed. Appearance of corrugated contributes to the growth of surface profiles (Fig. 8b).

Development of such structure on exposed surfaces is probably caused by presence of tensile residual stresses of (450–500 MPa) together with excess complex of interstitial atoms (δB <0 always for WTa5 targets) and large number of dislocation (B \approx 1.2 \times 10⁻² rad and practical not change).

4. Conclusions

Comparative experimental studies of the macroscopic erosion of double forging pure tungsten and tungsten–tantalum alloy samples have been performed with a quasi-stationary plasma accelerator QSPA Kh-50. The heat loads on the surface were $0.45\,\mathrm{MJ/m^2}$ (i.e., below the melting threshold) or $0.75\,\mathrm{MJ/m^2}$ (i.e., between the melting- and evaporation-threshold). The plasma pulse duration amounted to about $0.25\,\mathrm{ms}$.

With heat load below melting threshold macro cracks network forms only in case of initial target temperatures about RT on exposed surface of pure tungsten. Corrugated structures appear on

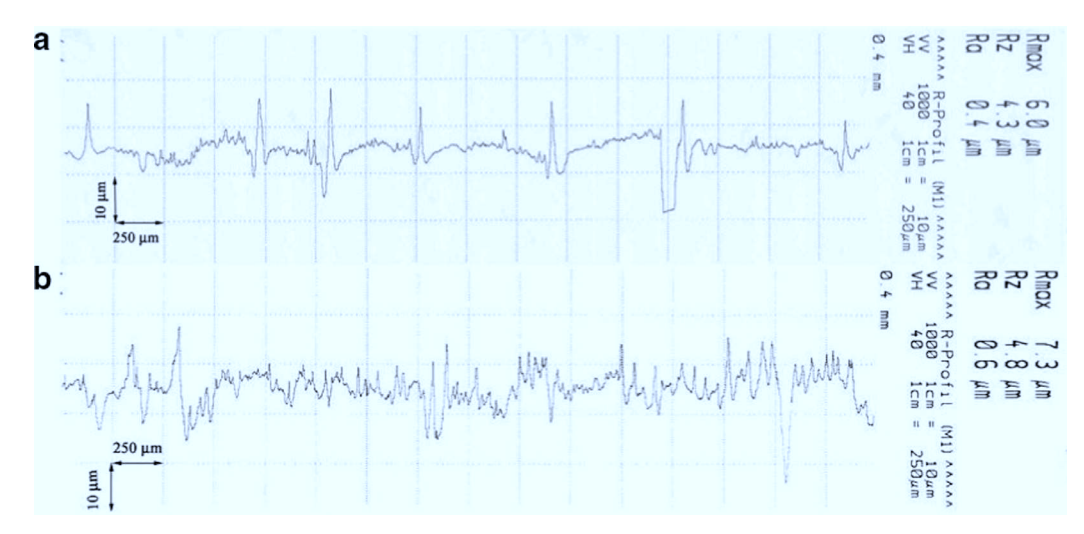


Fig. 6. Surface profiles of W (a) and WTa5 (b) development in the course of 100 plasma exposures, heat load Q=0.75 MJ/m2.

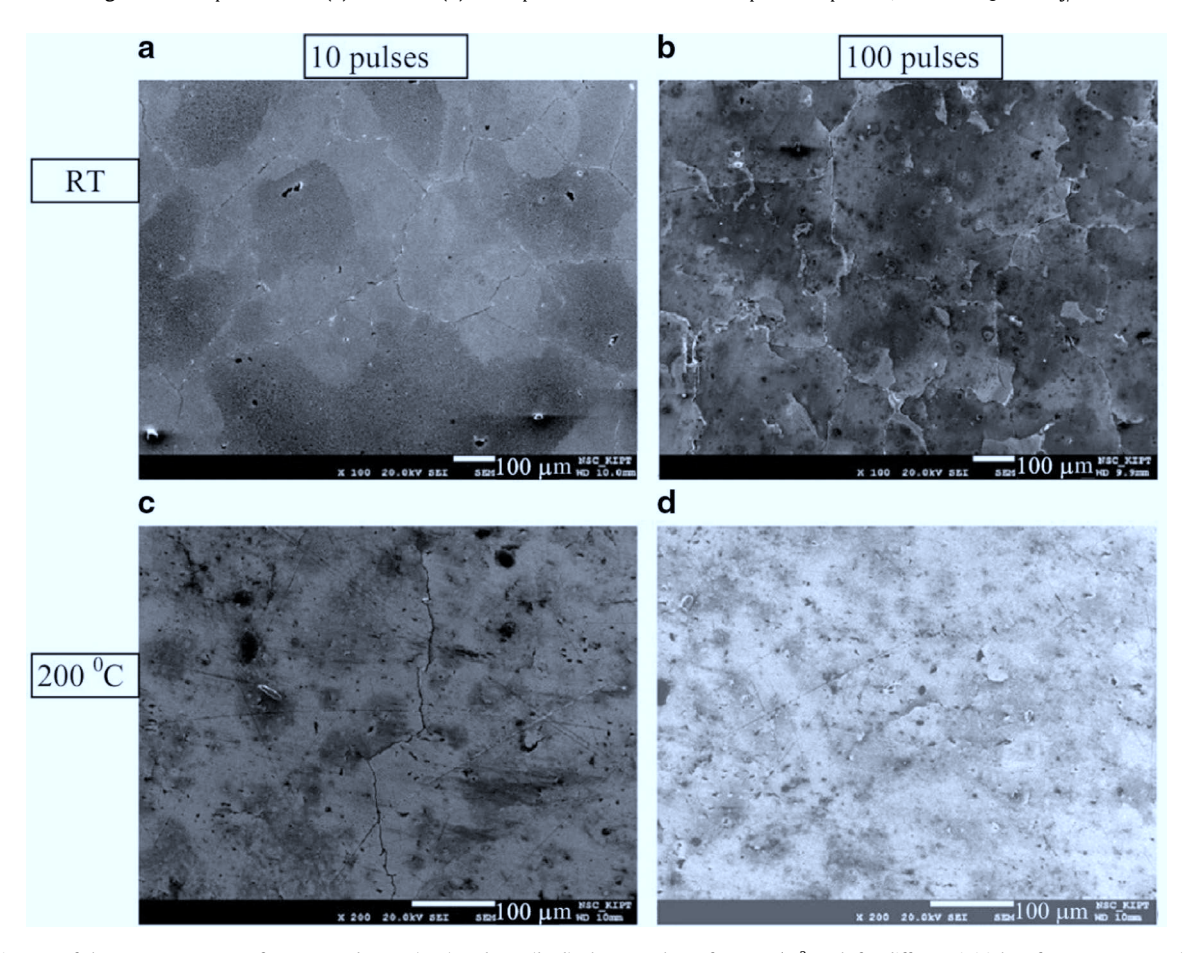


Fig. 7. SEM images of the pure tungsten surface exposed to 10 (a, c) and 100 (b, d) plasma pulses of $0.45 \, MJ/m^2$ each for different initial surface temperature (Tin): Tin =RT (a,b) and Tin= $200 \, ^{\circ}$ C (c,d). The length of the white marker line is $100 \, \mu m$.

preheated surface of tungsten-tantalum alloy after first pulses and develop with increasing of number of pulses. Further evolution of cracks network and corrugated structure is accompanied by increase of crack width and swelling of cracks edges.

Networks of micro- and macro-cracks develop on surfaces of pure tungsten and tungsten-tantalum alloy as a result of surface irradiation with heat load above the melting threshold. Surface modification and development of cracks led to increases of roughness of exposed surfaces.

The micro deformations of pure tungsten and tungstentantalum alloy are similar for targets exposed in similar conditions. Residual stress grows with increase of energy load. Relaxation of stresses is observed with increasing of number of pulses. Melting of surface layer essentially adds to the relaxation of stresses and increasing of absolute value of diffraction line asymmetry. This may be explained by increase in the number of interstitial complexes, which is consistent with a slight increase in the lattice parameter.

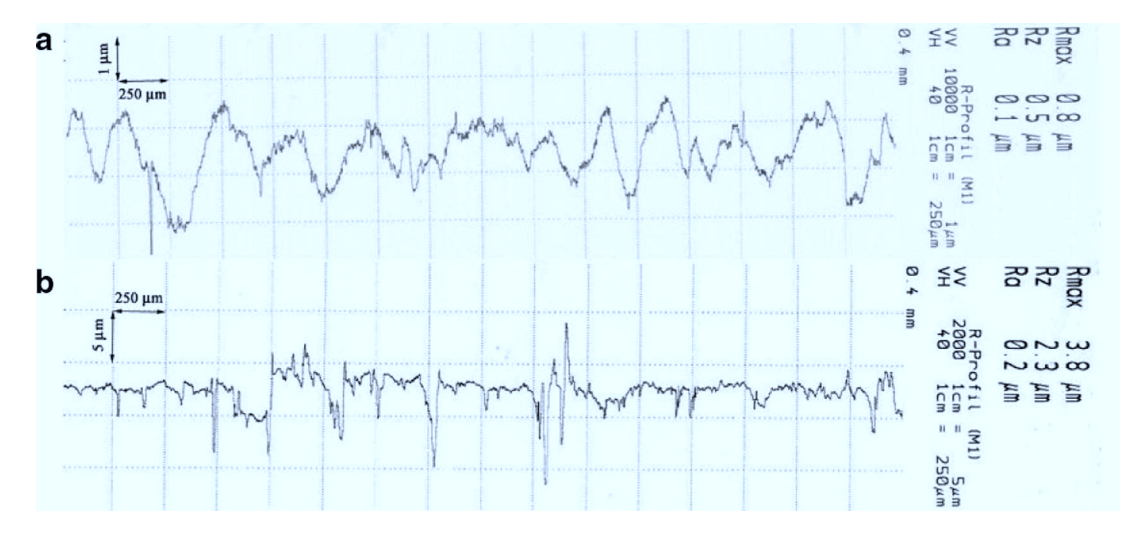


Fig. 8. Surface profiles of W (a) and WTa5 (b) development in the course of 100 plasma exposures, heat load Q=0.45 MJ/m².

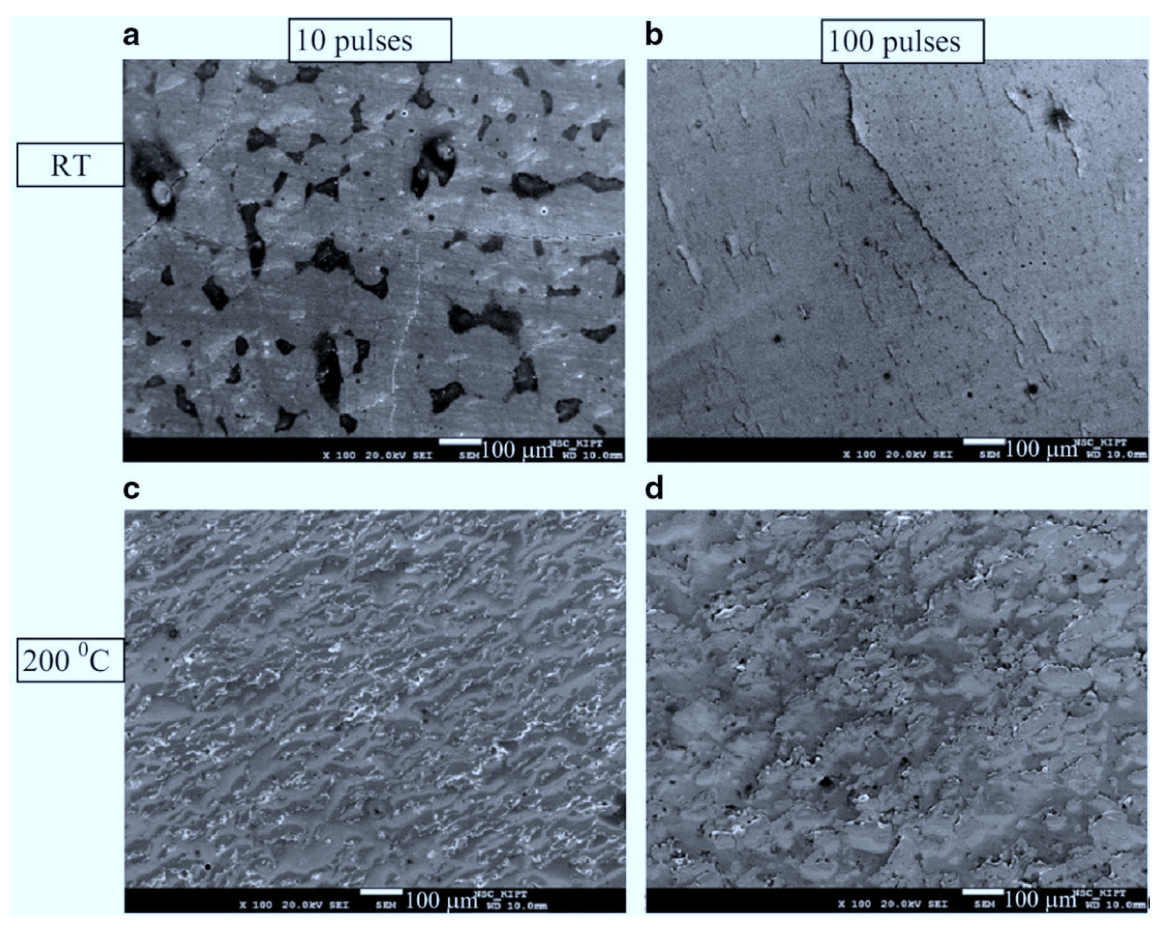


Fig. 9. SEM images of the WTa5 alloy surface exposed to 10 (a, c) and 100 (b, d) plasma pulses of 0.45 MJ/m^2 each for different initial surface temperature (Tin): Tin =RT (a,b) and Tin= $200 \, ^{\circ}\text{C}$ (c,d). The length of the white marker line is $100 \, \mu\text{m}$.

Acknowledgments

This work has been performed in part within IAEA CRP F1.30.13 and also partially supported by the STCU project #6057, and National Academy Science of Ukraine project Π -5/24-2015. The authors would like to acknowledge N.V. Kulik, V.V. Staltsov, S.I. Lebedev, P.V. Shevchuk for assisting in the experiments and also Dr. A.S. Kalchenko for assisting in imaging of surfaces with SEM.

References

- [1] M. Rieth, et al., J. Nucl. Mater. 442 (2013) S173-S180.
- [2] T. Hirai, et al., J. Nucl. Mater. 463 (2015) 1248–1251.
- [3] M. Wirtz, et al., Phys. Scr. T145 (2011) 014058.
- [4] N.S. Klimov, et al., Fusion Sci. Technol. 66 (2014) 118–124.
- [5] I.E. Garkusha, et al., J. Nucl. Mater. 415 (2011) S65–S69.[6] V.A. Makhlaj, et al., Phys. Scr. T159 (2014) 014024.
- [7] V.A. Makhlaj, et al., Phys. Scr. T161 (2014) 014024.
- [8] I.E. Garkusha, et al., J. Phys.: Conf. Ser. 591 (2015) 012030.

- [9] I.E. Garkusha, et al., Fusion Sci. Technol. 65 (2) (2014) 186.
 [10] V.A. Makhlaj, et al., J. Nucl. Mater. 438 (2013) S233–S236.
 [11] M.A. Krivoglaz, X-Ray and Neutron Diffraction in Nonideal Crystals, Springer-Verlag, Berlin Heidelberg, 1996.

- [12] V.A. Makhlaj, et al., Phys. Scr. T138 (2009) 014060.
 [13] I.E. Garkusha, et al., Tech. Phys. 59 (2014) 1620–1625.
 [14] S.V. Bazdyreva, et al., Prob. At. Sci. Technol 94 (6) (2014) 48–51.